JOC The Journal of Organic Chemistry

Article

pubs.acs.org/joc

# Formation of 1,10-Phenanthroline-*N*,*N*′-dioxide under Mild Conditions: The Kinetics and Mechanism of the Oxidation of 1,10-Phenanthroline by Peroxomonosulfate Ion (Oxone)

Gábor Bellér,*[,†] Mária Szabó,[†] Gábor Lente,[‡] and István Fábián[‡]

[†]MTA-DE Homogeneous Catalysis and Reaction Mechanisms Research Group, University of Debrecen, H-4032 Debrecen, Egyetem tér 1, Hungary

[‡]Department of Inorganic and Analytical Chemistry, University of Debrecen, H-4032 Debrecen, Egyetem tér 1, Hungary

Supporting Information

**ABSTRACT:** This paper confirms the unexpected formation of 1,10-phenanthroline-*N*,*N*′-dioxide ($phenO_2$) when 1,10-phenanthroline (phen) is oxidized by peroxomonosulfate ion (PMS) in a neutral aqueous solution. The kinetics of oxidation of phen by PMS features a complex pH dependence. In 1.00 M $H_2SO_4$, 1,10-phenanthroline-mono-*N*-oxide (phenO) is the sole product of the reaction. The rate of the N-oxidation is highly dependent on pH with a maximum at pH ∼6.7. The formation of phenO occurs via two parallel pathways: the rate constant of the oxidation of phen ($k$ = 3.1 ± 0.1 $M^{-1}$ $s^{-1}$) is significantly larger than that of $Hphen^+$ [$k$ = (4.1 ± 0.3) × $10^{-3}$ $M^{-1}$ $s^{-1}$] because the two N atoms are open to oxidative attack in the deprotonated substrate while an internal hydrogen bond hinders the oxidation of the protonated form. With an excess of PMS, four consecutive oxidation steps were found in nearly neutral solutions. In the early stage of the reaction, the stepwise oxidation results in the formation of phenO, which is converted into $phenO_2$ in the second step. The formation of $phenO_2$ was confirmed by $^1$H NMR and ESI-MS methods. The results presented here offer the possibility of designing an experimental protocol for preparing $phenO_2$.

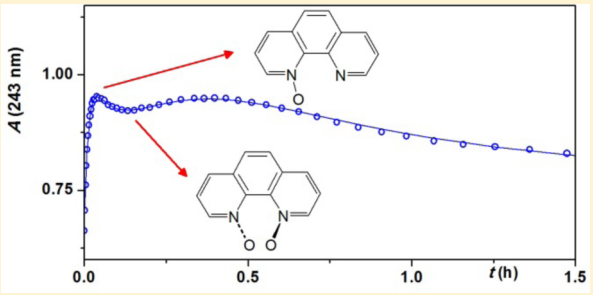


## INTRODUCTION

Peroxomonosulfate ion (PMS)[1] is an inexpensive and environmentally friendly replacement for other peroxo species (such as $H_2O_2$ or $S_2O_8^{2-}$) in oxidation procedures. It is a strong, two-electron oxidant, which is commercially available in the form of a triple salt ($2KHSO_5{\cdot}KHSO_4{\cdot}K_2SO_4$, Oxone). PMS is considered a green oxidant, and numerous inexpensive, high-yield, and simple procedures have been developed, which make PMS an important reagent in organic chemistry.[2] There are several particularly interesting reactions of PMS: oxidation of alkanes in the absence of organic solvents,[3] oxidative transformations via umpolung of bromide,[4] syntheses of *o*-carboxyarylacrylic acids by oxidative cleavage,[5] and transition metal-free preparation of carbonyl-containing oxindoles.[6] Recently, the frequency of its use has also increased rapidly as a mild oxidizing agent in various industrial technologies such as wastewater treatment,[7] bleaching,[8] microetching,[9] etc. Detailed mechanistic studies of the oxidation reactions of PMS have been sporadic, although such studies provide valuable information about the reactive intermediates and may explore important aspects of preparative and industrial applications. Earlier, we have reported kinetic studies of the oxidation of various substrates by PMS.[10,11] We have shown that simultaneous oxidation of the central metal ion and the ligand leads to somewhat unusual kinetic patterns in the PMS–$Fe(phen)_3^{2+}$ system (phen being 1,10-phenanthroline).[12]

1,10-Phenanthroline is a well-known bidentate ligand that forms stable complexes with transition metal ions.[13] It has been utilized extensively in analytical procedures and enjoys undiminished popularity as a building block in supramolecular chemistry[14] and as a versatile starting compound in preparative organic chemistry.[15,16] Phen is a planar, rigid, hydrophobic, and electron-poor N-heteroaromatic ligand with specific structural features that control its coordination abilities and provide various application possibilities. Phen derivatives and their metal complexes have been used, for example, for cleaving DNA,[17] as a radiometric chemosensor,[18] as an additive in C–H arylation processes,[19] or as photoswitchable molecular devices.[20] In these systems, the mechanisms and products of the redox reactions of phen are of utmost relevance.

The oxidation of phen has been the subject of interest for more than 70 years.[21] Chemical[22−24] and electrochemical[25] oxidations typically lead to the dearomatization or opening of the middle ring. However, the use of peroxo compounds usually results in the N-oxidation of one of the nitrogen atoms.[15,26] *N*-Oxides of heterocycles have received much

**Received:** March 24, 2016
**Published:** May 26, 2016





DOI: 10.1021/acs.joc.6b00641
J. Org. Chem. 2016, 81, 5345−5353

attention because of their applicability as important intermediates in organic syntheses,[27] protecting groups,[28] ligands in metal complexes,[29] energetic materials,[30] and biologically relevant molecules.[31] Although exhaustive procedures using $H_2O_2$ in acetic acid (peracetic acid) or *m*-chloroperoxybenzoic acid (*m*-CPBA) readily give the di-*N*-oxide and tri-*N*-oxide of 2,2′-bipyridine[32,33] and 2,2′:6′,2″-terpyridine,[34] respectively, similar methods give only the mono-*N*-oxide (phenO) in the case of phen. The first report about the existence of 1,10-phenanthroline-*N*,*N*′-dioxide (phen$O_2$) dates to 1946,[21] but later it was shown that the synthesis results in the formation of only phenO. Other research groups also failed to prepare phen$O_2$ for a long time.[33,35] The unsuccessful attempts and false reports about the preparation of phen$O_2$ convinced Gillard to reject the existence of this compound and its complexes.[36]

The specific behavior of phen in oxidation reactions was explained by its rigid structure compared to the bipyridine derivatives and the limited space in the bay area of the molecule that cannot accommodate two oxygen atoms. Rozen and Dayan at last succeeded in preparing the dioxide by using a mixture of $F_2$, $H_2O$, and $CH_3CN$ in 1999.[37] Since the first synthesis, a couple of phen$O_2$ derivatives have been prepared.[38] However, until now, the only published method for the synthesis is the one described by Rozen and Dayan, and it is still the prevailing opinion that phen$O_2$ cannot be produced by the use of peroxo compounds. In this paper, we report a detailed kinetic study of the oxidation of phen by PMS in the pH range of 1−12. We confirm that in contrast to the generally accepted presumption, PMS is able to oxidize phen to the di-*N*-oxide under relatively mild conditions. The results presented here may open new ways for the preparation phen$O_2$ and its derivatives for various practical applications.

## RESULTS AND DISCUSSION

**Kinetics in Acidic Medium.** Typical spectral observations during the reaction of phen and PMS under highly acidic conditions are shown in Figure 1. When the reactants are mixed, the main features are the formation of a broad band in the range of 350−390 nm and the occurrence of isosbestic points at 300, 306, 314, and 322 nm.

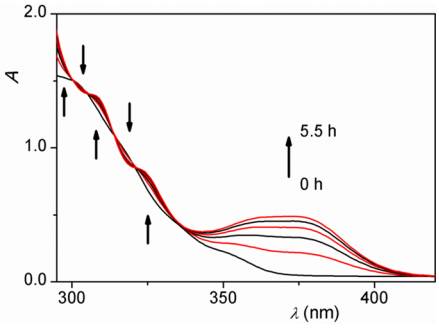


**Figure 1.** Spectral changes in the reaction of phen and PMS under strongly acidic conditions: $[PMS]_0$ = 27.4 mM, $[phen]_0$ = 0.234 mM, $[H_2SO_4]$ = 1.00 M, $t$ = 25.0 °C, path length = 1.000 cm, and time interval = 40 min.

Linear algebraic decomposition of the UV−vis spectra[39] showed that there are two independent absorbing species in the reaction, and these experimental results are consistent with a simple A → B process without detectable intermediates (Table S1). The two absorbing species are 1,10-phenanthroline and its oxidation product, 1,10-phenanthroline-mono-*N*-oxide. Under acidic conditions, $^1$H NMR and ESI-MS methods showed only the signals of the mono-*N*-oxide as the sole oxidation product, even at a large excess of the oxidant. Photometric studies confirm a 1:1 $Hphen^+$:PMS ratio in 1.0 M $H_2SO_4$ (Figure S1). The results confirm eq 1, which is in agreement with previous literature reports.[15,33,35]

$$Hphen^+ + HSO_5^- \rightarrow phenO + SO_4^{2-} + 2H^+ \quad (1)$$

At neutral pH, the 1:1 stoichiometry is valid only when the oxidant is used in substoichiometric amounts or in slight excess, but further oxidation reactions occur in the presence of a larger excess of PMS.

Under acidic conditions, the oxidation kinetics was studied at 375 nm using an excess of PMS (Figure S2) as well as stoichiometric conditions. The kinetic curves could be fitted to a single-exponential function when pseudo-first-order conditions were applied (≥20-fold excess of PMS over phen). The pseudo-first-order rate constant is a linear function of the concentration of PMS with zero intercept (Figure S3) and independent of the initial phen concentration at a constant $[PMS]_0$. Thus, the reaction follows overall second-order kinetics as shown in eq 2.

$$v = k_{1a}[Hphen^+][HSO_5^-] \quad (2)$$

The second-order rate constant obtained under pseudo-first-order conditions is in excellent agreement with that estimated on the basis of kinetic curves recorded at close to stoichiometric concentration ratios of the reactants (Table S2). In the latter experiments, a 1−5-fold excess of PMS was used and the experimental traces were directly fitted to eq 3:[40]

$$A_t = A_\infty + \frac{\Delta \times (A_0 - A_\infty)}{[PMS]_0 e^{(k_{1a} t \Delta)} - [phen]_0} \quad (3)$$

where $A_0$ and $A_\infty$ are the initial and final absorbance, respectively, $A_t$ is the absorbance at a given reaction time $t$, and $\Delta = [PMS]_0 - [phen]_0$. The calculated second-order rate constant in highly acidic medium is $k_{1a} = (6.4 \pm 0.2) \times 10^{-3}$ $M^{-1}$ $s^{-1}$.

**pH and Temperature Dependence.** The effect of pH on the initial rate of the reaction was investigated in the pH range of 1−12 by using different buffer systems [$H_3PO_4/H_2PO_4^-$, $CH_3COOH/CH_3COO^-$, $H_2PO_4^-/HPO_4^{2-}$, and $B(OH)_3/B(OH)_4^-$] and NaOH. To minimize the interference of the second-order decomposition of PMS in basic medium,[41] the further oxidation of phenO, or any possible side reaction, the initial rate method was used and PMS was applied at relatively low concentrations (~5 mM, ~20-fold excess).

The initial rate is defined as the initial rate of absorbance increase at 375 nm, which is due to the formation of phenO. The reactant (phen) and the product (phenO) are involved in acid−base equilibria in the studied pH region, which affects the absorbance change. The molar absorptivities and the p$K_a$ values were determined by a combined pH potentiometric and spectrophotometric method, in which the UV−vis spectra of phen and phenO were recorded as a function of pH (Figure S4a,b).[42] The p$K_a$ of the *N*-oxide was found to be considerably higher than that of phen (Table 1), which is probably due to the stabilizing effect of an intramolecular hydrogen bond formed in $Hphen^+$ (Scheme 1).[15] The literature value of p$K_a$ of phenO, 6.63 at 22 °C,[15] is somewhat smaller than the one reported here. Such a difference is not unexpected considering


DOI: 10.1021/acs.joc.6b00641
J. Org. Chem. 2016, 81, 5345−5353

**Table 1. Thermodynamic and Kinetic Parameters for the Reaction between phen($H^+$) and $HSO_5^-$**

| parameter | value | unit | remark |
|---|---|---|---|
| $k_{1a}$ | $(4.1 \pm 0.3) \times 10^{-3}$ | $M^{-1}$ $s^{-1}$ | 25.0 °C, 1.00 M $NaNO_3$[a] |
| | $(6.4 \pm 0.2) \times 10^{-3}$ | $M^{-1}$ $s^{-1}$ | 25.0 °C, 1.00 M $H_2SO_4$[a] |
| $\Delta S^{\ddagger}$ | $-133.8 \pm 1.1$ | J $mol^{-1}$ $K^{-1}$ | $Hphen^+ + HSO_5^-$ (eq 1a)[a] |
| $\Delta H^{\ddagger}$ | $45.7 \pm 0.3$ | kJ $mol^{-1}$ | $Hphen^+ + HSO_5^-$ (eq 1a)[a] |
| $k_{1b}$ | $3.1 \pm 0.1$ | $M^{-1}$ $s^{-1}$ | 25 °C, 1.00 M $NaNO_3$[a] |
| $\Delta S^{\ddagger}$ | $-133.5 \pm 3.0$ | J $mol^{-1}$ $K^{-1}$ | phen + $HSO_5^-$ (eq 1b)[a] |
| $\Delta H^{\ddagger}$ | $30.6 \pm 0.9$ | kJ $mol^{-1}$ | phen + $HSO_5^-$ (eq 1b)[a] |
| $pK_a^{HSO_5}$ | $8.41 \pm 0.03$ | | fitting the data to eq 6[a] |
| | 8.43 | | from ref 11 |
| $pK_a^{phen}$ | $5.12 \pm 0.03$ | | fitting the data to eq 6[a] |
| | $5.12 \pm 0.01$ | | pH-metric titration[a] |
| | $5.13 \pm 0.01$ | | pH-metric–spectrophotometric titration[a] |
| | 5.08 | | from ref 43 |
| $pK_a^{phenO}$ | $7.30 \pm 0.02$ | | pH-metric–spectrophotometric titration, 25.0 °C, $I$ = 1.00 M[a] |
| | $6.97 \pm 0.02$ | | NMR titration, 25.0 °C, $I$ = 0.20 M[a] |
| | 6.63 | | from ref 15; 22 °C, $I$ < 0.1 M |

[a]From this work.

**Scheme 1. Intramolecular Hydrogen Bond in $Hphen^+$ ($phen \cdot H_3O^+$) and $HphenO^+$**

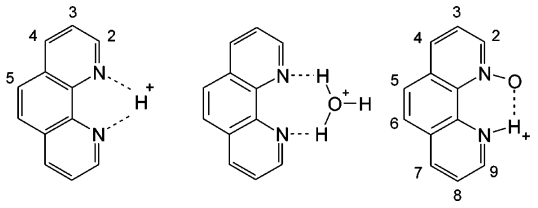

that the previous work was conducted at a considerably lower total ionic strength ($I$ < 0.1 M).

The peaks in the $^1H$ NMR spectra of $Hphen^+$ shift upfield with an increase in pH (Figure S5), and the very same pattern was observed with $HphenO^+$ (Figure 2). Simultaneous evaluation of all the $\delta$ versus pH curves (Figure S6) resulted in a $pK_a$ of 6.97 ± 0.02 ($I$ = 0.2 M) for $HphenO^+$.

It was assumed that eq 2 is valid over the entire pH range, and the experimental initial rates were converted into pseudo-second-order rate constants ($k_1$) by using the difference in the apparent molar absorptivities of the reactant (phen) and the product (phenO) at a given pH. The pseudo-second-order rate constant of the reaction shows a distinct pH profile with a maximum at pH ~6.7 (Figure 3). Such a pH profile can be interpreted by considering the protolytic equilibria of the reactants (eqs 4 and 5).

$$Hphen^+ \rightleftharpoons phen + H^+;\ K_a^{phen} = \frac{[phen][H^+]}{[phenH^+]} \quad (4)$$

$$HSO_5^- \rightleftharpoons SO_5^{2-} + H^+;\ K_a^{HSO_5} = \frac{[SO_5^{2-}][H^+]}{[HSO_5^-]} \quad (5)$$

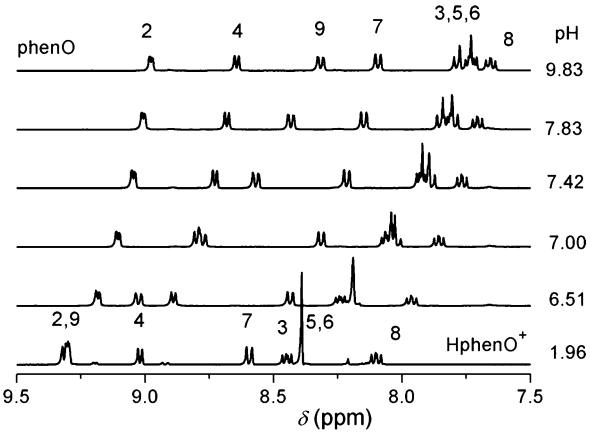


**Figure 2.** pH dependence of the $^1H$ NMR spectra of phenO in $H_2O$: $[phenO]_{tot}$ = 5.5 mM, $I$ = 0.20 M, and $t$ = 25.0 °C. The numbering of phenO is in accordance with Scheme 1.

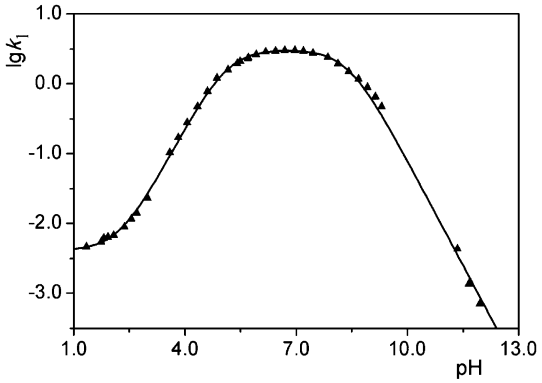


**Figure 3.** pH dependence of the pseudo-second-order rate constant ($k_1$, $M^{-1}$ $s^{-1}$) of the reaction of phen and PMS: $[PMS]_0$ = 4.8 mM, $[phen]_0$ = 0.250 mM, $I$ = 1.00 M ($NaNO_3$), $[buffer]_{tot}$ = 50.0 mM, $t$ = 25.0 °C, and $\lambda$ = 375 nm. The line is the result of a nonlinear fit to eq 6.

where $K_a^{phen}$ and $K_a^{HSO_5}$ are the acid dissociation constants of $Hphen^+$ and $HSO_5^-$, respectively.

In principle, the redox reaction may proceed via the following parallel reaction paths:

$$Hphen^+ + HSO_5^- \rightarrow phenO + SO_4^{2-} + 2H^+ \quad k_{1a} \quad (1a)$$

$$phen + HSO_5^- \rightarrow phenO + SO_4^{2-} + H^+ \quad k_{1b} \quad (1b)$$

$$Hphen^+ + SO_5^{2-} \rightarrow phenO + SO_4^{2-} + H^+ \quad k_{1c} \quad (1c)$$

$$phen + SO_5^{2-} \rightarrow phenO + SO_4^{2-} \quad k_{1d} \quad (1d)$$

In agreement with the kinetic results in sulfuric acid, $k_1$ does not converge to zero under acidic conditions, confirming that reaction 1a is operative at low pH. The protolytic equilibria between the acidic and basic forms of the reactants are expected to be extremely fast; thus, reactions 1b and 1c are indistinguishable because of proton ambiguity.[40] Under alkaline conditions, $k_1$ shows a linear correlation with a decreasing $H^+$ concentration and practically becomes zero as the pH increases. It confirms that reaction 1d can be neglected. In accordance with these considerations, the pH dependence of $k_1$ is given by the following equation (eq 6):



DOI: 10.1021/acs.joc.6b00641
J. Org. Chem. 2016, 81, 5345–5353

$$k_1 = \frac{v_0}{[\text{phen}]_0[\text{PMS}]_0\Delta\varepsilon} = \frac{k_{1a}[H^+]^2 + \kappa[H^+]}{(K_a^{\text{phen}} + [H^+])(K_a^{\text{HSO}_5} + [H^+])} \quad (6)$$

where

$$\kappa = k_{1b}K_a^{\text{phen}} + k_{1c}K_a^{\text{HSO}_5}$$

The experimental data were fitted to eq 6 by using a nonlinear least-squares algorithm and proportional weighting (the weight for $k_1$ is $k_1^{-2}$ at each pH).[40]

The estimated values for $pK_a^{\text{phen}}$ and $pK_a^{\text{HSO}_5}$ are in good agreement with the literature results at similar ionic strengths (Table 1). The existence of $H(phen)_2^+$ has also been reported previously.[43,44] The formation of this species was neglected because it is formed at concentrations of phen considerably higher than those used in this study. Our spectrophotometric, pH-metric, and kinetic studies did not indicate the presence of $H(phen)_2^+$ either.

The estimated value of $k_{1a}$ is somewhat smaller than that found in 1.00 M $H_2SO_4$ (Table 1). This difference is probably due to medium effects. In 1.00 M $H_2SO_4$, the ionic strength and ionic atmosphere are different from those in 1.00 M $NaNO_3$ used in the pH-dependent study.

The pH profile confirms that the dominant reaction path includes the acidic form of one reactant and the basic form of the other. The proton ambiguity cannot be resolved by the fitting procedure itself; only the $\kappa$ value of $(2.35 \pm 0.12) \times 10^{-5}$ $s^{-1}$ can be estimated. However, the contributions of the two concurrent reactions (1b and 1c) can be estimated by considering the redox chemistry of the reactants. According to earlier results, $HSO_5^-$ is much more reactive than the fully deprotonated form of PMS.[10,11] The protonation of phen is expected to hinder N-oxidation, making the protonated form of the substrate less reactive in such reactions. Thus, it is a reasonable assumption that reaction 1c makes a minor contribution to the overall process and the main reaction occurs between phen and $HSO_5^-$ (reaction 1b). This conclusion is also supported by the observation that the reaction rate at pH ~6.6 is practically independent of the ionic strength at constant initial reactant concentrations (Table S3), as expected when the charge product of the reactants is zero. When the second term of $\kappa$ is omitted, the rate constant of reaction 1b can be estimated: $k_{1b} = 3.1 \pm 0.1$ $M^{-1}$ $s^{-1}$, which is nearly 3 orders of magnitude larger than $k_{1a}$. Statistical factors (the number of oxidizable N atoms) and the differences in the electrostatic interactions are expected to have relatively small effects on the reactivities of the two forms. Thus, the sluggishness of $Hphen^+$ compared to phen in N-oxidation is probably a consequence of the formation of an internal hydrogen bond in the protonated form (Scheme 1),[45] which efficiently hinders the attack of the oxidant on the N atoms.

The temperature dependencies of reactions 1a and 1b were studied in the range of 10−40 °C under pseudo-first-order conditions. Deviation from the first-order behavior, i.e., secondary reactions, was not observed even at high temperatures. The second-order rate constants were calculated as described above. In a strongly acidic solution (1.00 M $H_2SO_4$), both reactants are fully protonated and the oxidation proceeds only via reaction 1a (cf. eq 6). Thus, the temperature dependence of the protolytic equilibria can be neglected. Such a simplification is not applicable for reaction 1b even if it is studied under slightly acidic conditions (pH ~4.4). While PMS is present as $HSO_5^-$, the concentrations of $Hphen^+$ and phen are comparable and the concentration ratio of these species might change as a function of temperature. The temperature dependence of the $pK_a$ of $Hphen^+$ was determined by conventional pH-metric titration.[46] Temperature-dependent kinetic studies were conducted in acetate buffer because its $pK_a$ is practically independent of the temperature in the studied range.[47] In each kinetic run, the pH was measured and the $[Hphen^+]/[phen]$ ratio was calculated. The value of $k_{1b}$ was determined on the basis of eq 6 by also taking into account the contribution of reaction 1a (Table S4).

The parameters of activation were estimated by fitting the experimental rate constants to the Eyring equation (eq 7) using proportional weighting (Figure S7):

$$k = \frac{k_b T}{h} \exp\left(\frac{\Delta S^{\ddagger}}{R}\right) \exp\left(-\frac{\Delta H^{\ddagger}}{RT}\right) \quad (7)$$

where $k$ is the second-order rate constant ($k_{1a}$ or $k_{1b}$), $k_b$ is Boltzmann's constant, $h$ is Planck's constant, $R$ is the universal gas constant, and $\Delta S^{\ddagger}$ and $\Delta H^{\ddagger}$ are the entropy and enthalpy of activation, respectively. The results are listed in Table 1. The activation entropies are essentially identical large negative values. In earlier studies, it was concluded that large negative entropies of activation are characteristic of $2e^-$ oxidation reactions of PMS, which involves O atom transfer.[10,48] Thus, we conclude that the oxidations of phen and $Hphen^+$ by $HSO_5^-$ proceed via concerted heterolytic O−O bond cleavage and N−O bond formation.

**Formation of 1,10-Phenanthroline-*N*,*N*′-dioxide under Neutral Conditions.** Treatment of the colorless aqueous solution of phen with an equivalent amount of PMS at pH ~6.6 results in the formation of phenO, turning the mixture light yellow (featuring a broad absorbing band between 360 and 380 nm). In the presence of a slight excess of phen, the final absorbance remains stable (Figure S8), proving that phenO is stable within the observed time interval.

Upon the addition of an equivalent amount of PMS to the solution of phenO, the yellowish color intensifies and the absorbance maximum also shifts toward lower wavelengths (360 nm) under neutral conditions. The spectral change is most likely due to the oxidation of phenO by PMS to 1,10-phenanthroline-*N*,*N*′-dioxide ($phenO_2$). Such a reaction does not occur in an acidic solution where the monoxide is fully protonated. Presumably, the formation of an internal hydrogen bond in $HphenO^+$ (Scheme 1) shields the second N atom and prevents its oxidation even when the oxidant is present in a large excess. The noted pH effect serves as strong indirect evidence that the second nitrogen atom is involved in the process and the formation of $phenO_2$ occurs.

The significance of pH in the oxidation of phenO is also demonstrated by the following experiment. The reaction of phen and PMS was initiated at pH 2.2 in the presence of an ~24-fold excess of oxidant, and the formation of phenO was observed in a first-order process. After the reaction was complete (~15 h), a pH jump to 6.4 was induced by the addition of a sufficient amount of $H_2PO_4^-/HPO_4^{2-}$ buffer to the reaction mixture. First, the absorbance slightly decreased because of dilution and the deprotonation of $HphenO^+$, which has a molar absorptivity higher than that of phenO at 375 nm. This absorbance change was followed by an immediate increase as a result of $phenO_2$ formation (Figure 4). After reaching a



DOI: 10.1021/acs.joc.6b00641
J. Org. Chem. 2016, 81, 5345−5353

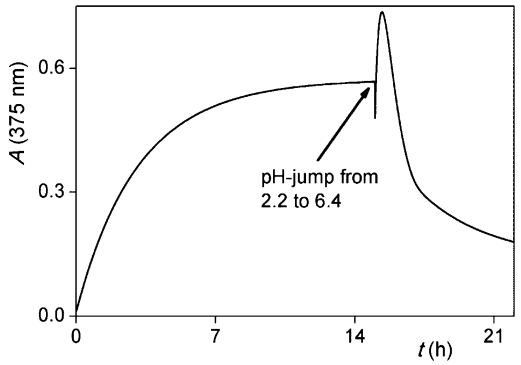


**Figure 4.** Kinetic trace demonstrating the effect of pH on the oxidation of phenO by PMS: $[phen]_0$ = 0.256 mM, $[PMS]_0$ = 6.10 mM, and $pH_{initial}$ = 2.2 (set by $HClO_4$). The pH jump was triggered by the addition of 50 $\mu$L of 0.5 M $Na_2HPO_4$ to 2 mL of the reaction mixture. Concentrations after dilution: [phen] = 0.250 mM, [PMS] = 5.95 mM, $[phosphate]_{tot}$ = 1.22 × $10^{-2}$ M, pH 6.4, $t$ = 25.0 °C, $\lambda$ = 375 nm, and path length = 1.000 cm.

maximum, the absorbance falls, indicating that $phenO_2$ is oxidized further. Assuming similar pH profiles for the rates of the oxidation of phen and phenO, we find the maximal rate is expected at pH ∼7.8 in the case of phenO.

The formation of $phenO_2$ was proven by two independent methods. The ESI-MS spectrum of the reaction mixture of phen and PMS in neutral medium features two intense peaks at $m/z$ 213.06 and 235.04 that belong to $HphenO_2^+$ and $\{Na\cdot phenO_2\}^+$, respectively (Figure S9a,b).

$^1$H NMR studies were also conducted to obtain detailed information about the primary and secondary oxidation products. Tuning the NMR instrument for recording time-dependent spectra requires several minutes during which the oxidation reaction progresses. Consequently, the very beginning of the reaction cannot be monitored by this technique in this system. Typical $^1$H NMR spectra as a function of time are shown in Figure 5A, and the variation of the corresponding peak intensities for phen and phenO is shown in Figure 5B.

The time resolution was not satisfactory for monitoring the formation of $phenO_2$; thus, a different approach was applied to identify the secondary oxidation product. First, phenO was produced in the reaction of phen with a stoichiometric amount of PMS, and then different amounts of the oxidant were added to phenO and the $^1$H NMR spectra of the spent reaction mixtures recorded. Figure 6 shows the consumption of phenO (denoted by B) and the formation of $phenO_2$ (denoted by C) as the amount of PMS is increased. According to earlier results,[37] the two oxygen atoms force the aromatic skeleton out of planarity and give a helical character to the molecule, resulting in a somewhat asymmetrical structure. Because of this feature, the protons in the two halves of $phenO_2$ are not entirely identical, and as a consequence, more than four sets of peaks are observed in the spectrum.

To the best of our knowledge, there is only one report about the formation of $phenO_2$ in the literature, when a HOF/$CH_3CN$ mixture was used as the oxidant.[37] The results presented here confirm that there is a straightforward way to generate $phenO_2$ in aqueous solution without using extreme conditions. Apparently, the key to solving the problem is the use of the appropriate (neutral) pH. However, the properties of the oxidant are also important. The oxidations of phen with strong oxidizing agents such as $O_3$, $H_2O_2$, $S_2O_8^{2-}$, and $MnO_4^-$

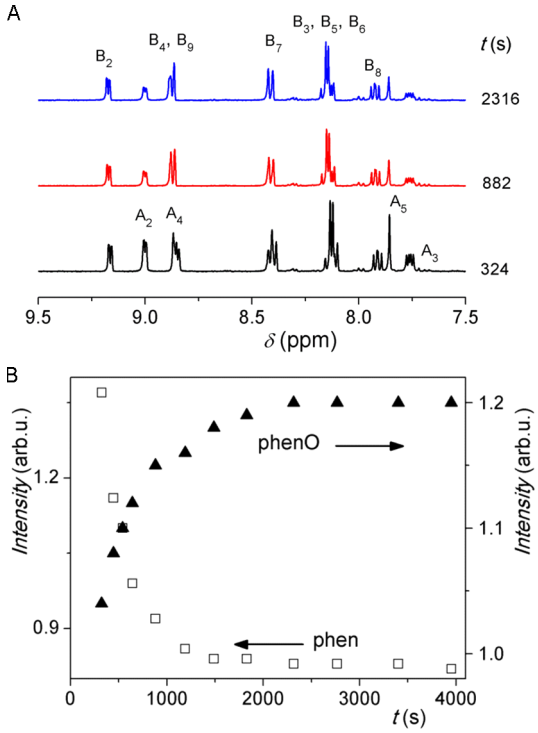


**Figure 5.** NMR study of the formation of phenO in neutral medium: [phen] = 3.0 mM, [PMS] = 3.0 mM, $[phosphate]_{tot}$ = 17 mM, pH 7.0, and $t$ = 25.0 °C. (A) Time-dependent $^1$H NMR spectra for the reaction of phen with an equivalent amount of PMS. The assignment of the peaks of phen (A) and phenO (B) is based on the numbering of Scheme 1. Note that the signals denoted by $A_4$, $B_4$, and $B_9$ overlap. (B) Intensities of the $^1$H NMR peaks as a function of time during the reaction. The plot is shown for the peaks of phen ($A_2$, $\delta$ = 8.98) and phenO ($B_2$, $\delta$ = 9.17).

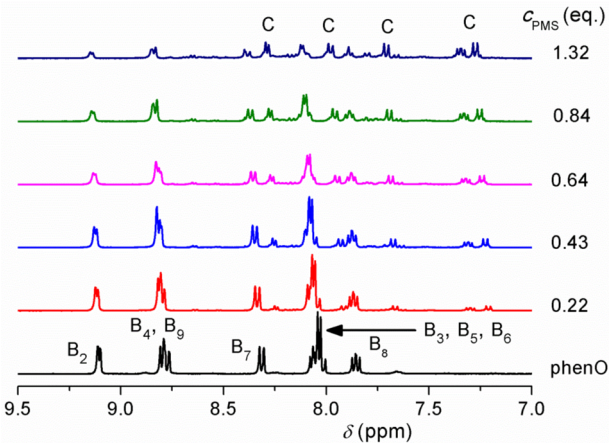


**Figure 6.** NMR study of the formation of $phenO_2$ in neutral medium: [phenO] = 5.5 mM, $[phosphate]_{tot}$ = 220 mM, pH 7.0, and $t$ = 25.0 °C. The bottom spectrum shows the spectrum of phenO in the absence of PMS. The rest of the spectra were recorded after the addition of the given amount of PMS and after the reaction had been allowed to reach completion. The assignment of the peaks of phenO (B) is based on the numbering of Scheme 1.

were attempted under neutral conditions, but these attempts failed to produce $phenO_2$.

**Kinetics of the Overall Oxidation Reaction under Nearly Neutral Conditions.** In an excess of the substrate, the oxidation reaction yields only phenO in a first-order process at



DOI: 10.1021/acs.joc.6b00641
J. Org. Chem. 2016, 81, 5345−5353

neutral pH (Figure S8). When an excess of PMS is applied, the spectral changes indicate a multistep process (Figure S10). To broaden the usable wavelength range, $NaNO_3$ was discarded and only $H_2PO_4^-/HPO_4^{2-}$ buffer was applied to set both the pH and the ionic strength. Kinetic traces at several selected wavelengths clearly indicate a complex kinetic pattern (Figure S11).

Singular-value decomposition analysis was used to determine the number of independent absorbing species in the reaction mixtures using the spectra in the wavelength range of 200−400 nm.[39] When the method was applied for gradually increasing reaction times, the number of absorbing species increases to 5 (Table S5). Four well-defined phases can be distinguished in some of the kinetic curves; thus, the new absorbing components are presumably produced in consecutive processes. Detailed kinetic studies were conducted at 243 nm, where the four subsequent phases of the reaction are clearly separated by the three extrema in the kinetic traces (Figure 7).

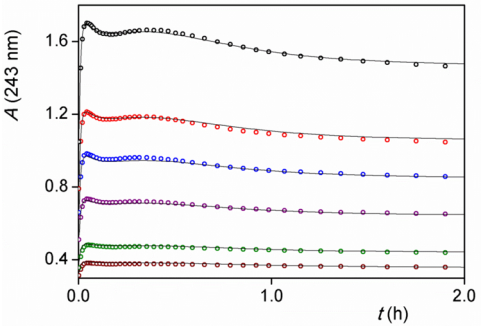


**Figure 7.** Experimental kinetic curves recorded in the reaction between phen and PMS in nearly neutral medium. Circles denote experimental data. Only 2% of the recorded points are shown for the sake of clarity. Lines show the results of the global fit to the model described by eqs 1 and 8−11: $[PMS]_0$ = 9.77 mM, $[phen]_0$ = 7.62, 12.7, 25.4, 38.1, 50.8, and 76.2 $\mu$M in order of increasing absorbance, $[phosphate]_{tot}$ = 1.01 × $10^{-1}$ M, pH 6.7, $t$ = 25.0 °C, $\lambda$ = 243 nm, and path length = 1.000 cm.

The noted effects were studied as a function of the concentrations of the two reactants (both of them were changed by 1 order of magnitude). As seen in Figure 7, the maxima and minima of the curves practically occur at the same reaction time when the initial concentration of phen is changed. This implies that the reaction order with respect to phen and its derivatives produced in the consecutive reactions is one in all steps; otherwise, the positions of the extrema would depend on the concentration of the limiting reactant. When the nearly constant contribution of PMS (which is used in large excess) is subtracted from the detected absorbance and the corrected curves are divided by the total concentration of phen, the normalized traces are practically identical within the limits of experimental error (Figure S12). This confirms again the first-order dependence of the subsequent reaction steps on phen and its oxidized derivatives.

The kinetic curves recorded under different initial conditions were simultaneously evaluated by considering the reactions of Scheme 2. The kinetic model consists of second-order oxidation steps and also includes the second-order decomposition of PMS (eqs 1 and 8−11). The contribution of this process to the consumption of PMS cannot be ignored completely at the applied pH (6.7).[41] Because the decomposition reaction is second order in PMS, it has a more profound effect when the initial concentration of the oxidant is relatively high.

$$\text{phen} + HSO_5^- \rightarrow \text{phenO} + SO_4^{2-} + H^+;$$

$$v = k_1[\text{phen}][\text{PMS}]$$

$$\text{phenO} + HSO_5^- \rightarrow \text{phenO}_2 + SO_4^{2-} + H^+;$$

$$v = k_8[\text{phenO}][\text{PMS}] \quad (8)$$

$$\text{phenO}_2 + HSO_5^- \rightarrow \text{I};\ v = k_9[\text{phenO}_2][\text{PMS}] \quad (9)$$

$$\text{I} + HSO_5^- \rightarrow \text{P};\ v = k_{10}[\text{I}][\text{PMS}] \quad (10)$$

$$HSO_5^- + SO_5^{2-} \rightarrow 2SO_4^{2-} + O_2 + H^+ \quad (11)$$

$$v = -\frac{1}{2} \times \frac{d[\text{PMS}]}{dt} = k_{11}[\text{PMS}]^2$$

The kinetic model is rather complex, and an explicit expression is not available for fitting the experimental kinetic traces. Thus, a comprehensive evaluation method that numerically solves the corresponding differential equation system and simultaneously fits the kinetic traces by using a nonlinear least-squares algorithm was used.[49]

Eleven parameters were used in these calculations: five rate constants and six molar absorptivities. Two rate constants ($k_1$ and $k_{11}$) and three molar absorption coefficients ($\varepsilon$ for phen, phenO, and PMS) were determined in independent experiments and were fixed, and the rest of the parameters ($k_8$, $k_9$, $k_{10}$, and $\varepsilon$ for $phenO_2$, an intermediate, and the product) were allowed to float. The estimated parameters are listed in Table 2.

It should be noted that these results were obtained at pH 6.7 and the pH dependencies of the corresponding parameters were not investigated in the overall process. However, it is a plausible assumption that the rate of the individual reaction steps and the corresponding kinetic parameters are pH-dependent: in the case of $k_1$, $k_8$, and $k_{11}$, the pH dependency is confirmed in this study or was previously,[41] and $k_9$ and $k_{10}$ might also change with pH.

**Scheme 2. Successive Oxidation Steps in the phen−PMS System under Nearly Neutral Conditions**[a]

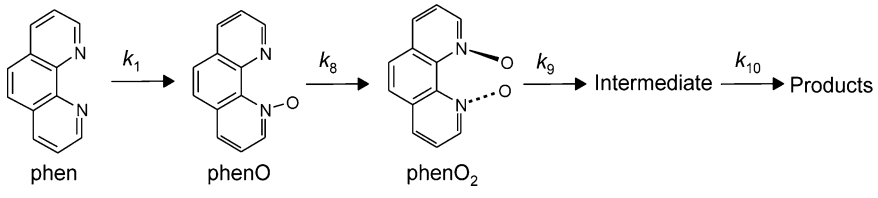


[a]Each rate constant corresponds to an oxidation step by PMS, which is used in excess.



DOI: 10.1021/acs.joc.6b00641
J. Org. Chem. 2016, 81, 5345−5353

**Table 2. Kinetic Parameters Resulting from Globally Fitting the Kinetic Data of the Oxidation of phen by PMS[a]**

| parameter | value | unit |
|---|---|---|
| $k_1$* | 2.97 | $M^{-1}$ $s^{-1}$ |
| $k_8$ | $(4.2 \pm 0.3) \times 10^{-1}$ | $M^{-1}$ $s^{-1}$ |
| $k_9$ | $(1.7 \pm 0.2) \times 10^{-1}$ | $M^{-1}$ $s^{-1}$ |
| $k_{10}$ | $(4.5 \pm 0.4) \times 10^{-2}$ | $M^{-1}$ $s^{-1}$ |
| $k_{11}$* | $2.5 \times 10^{-4}$ | $M^{-1}$ $s^{-1}$ |
| $\varepsilon_{PMS}$* | 25.0 | $M^{-1}$ $cm^{-1}$ |
| $\varepsilon_{phen}$* | $8.05 \times 10^{3}$ | $M^{-1}$ $cm^{-1}$ |
| $\varepsilon_{phenO}$* | $2.10 \times 10^{4}$ | $M^{-1}$ $cm^{-1}$ |
| $\varepsilon_{phenO_2}$ | $(1.7 \pm 0.1) \times 10^{4}$ | $M^{-1}$ $cm^{-1}$ |
| $\varepsilon_{int}$ | $(2.0 \pm 0.2) \times 10^{4}$ | $M^{-1}$ $cm^{-1}$ |
| $\varepsilon_{prod}$ | $(1.5 \pm 0.1) \times 10^{4}$ | $M^{-1}$ $cm^{-1}$ |

[a]pH 6.7, $t$ = 25 °C, and $\lambda$ = 243 nm. Parameters marked with an asterisk are known from independent experiments and were held fixed during the fitting procedure.

Using the calculated rate constants and the spectral series recorded at pH 6.7, the spectra of absorbing species were calculated.[50] The spectra of phen, phenO, and $phenO_2$ are shown in Figure 8, and further spectra can be found in Figure S13. The simulated spectra of phen and phenO are in perfect agreement with those calculated from the known spectra of the protonated and deprotonated species (Figure S4a,b) at the given pH.

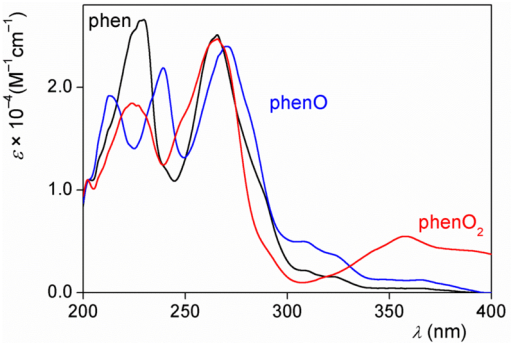


**Figure 8.** Calculated spectra of phen, phenO, and $phenO_2$ at pH 6.7 obtained by fitting a series of spectra to the model described by eqs 1 and 8–11.

By using the calculated rate constants, the concentration change of the species as a function of time can also be estimated (Figure S14). The shapes of these profiles (e.g., the maximal concentration of an intermediate) are intrinsically governed by the rate constants. The reaction time at which, e.g., PMS is completely consumed or phenO and $phenO_2$ reach maximal concentrations is determined by the initial concentrations of the reactants. With an initial 2:1 PMS:phen molar ratio at pH 6.7, a yield of 62–63% can be obtained for $phenO_2$ in the spent reaction mixture.

No attempt was made to isolate and identify the final products of the oxidation. The use of a large excess of oxidant probably results in the gradual cleavage of C–C and C–N bonds and the formation of smaller molecules due to the strong oxidizing ability of PMS. This assumption is supported by both ESI-MS and $^1$H NMR results. Mass spectrometric analysis of the reaction mixture containing a 7-fold excess of PMS over phen showed that there is no further increase in the $m/z$ values after the incorporation of the second oxygen atom.

$^1$H NMR studies also revealed that small peaks appear in the aliphatic region of the spectra when >2 equiv of PMS is added to phen. Both of these observations are in agreement with the opening of aromatic rings and gradual fragmentation of the parent molecule caused by the excess of oxidant. Such a feature of PMS is well-known and is taken advantage of in advanced oxidation processes (AOPs).[8]

## CONCLUSION

The oxidation of phen by PMS yields only $HphenO^+$ even in a large excess of the oxidant under acidic conditions. Presumably, an internal hydrogen bond inhibits further oxidation of the primary oxidation product. Deprotonation of $HphenO^+$ opens additional paths for oxidation. It was confirmed that one of the intermediates in this reaction is $phenO_2$, which was synthesized earlier using extreme conditions. The preparation of this species was not the objective of this work. However, the kinetic results presented here make it possible to design experimental protocols for such a purpose. Using suitable initial reactant concentrations (preferably a 2:1 PMS:phen molar ratio) or quenching the reaction by quick removal of the excess oxidant at the appropriate reaction time yields a spent reaction mixture with relatively high concentrations of $phenO_2$. Our ongoing experiments demonstrate very similar kinetic behavior with substituted phens. Thus, the production of the corresponding $phenO_2$ species seems to be feasible. The experimental observations are consistent with highly complex kinetic patterns under neutral conditions. A multistep kinetic model was confirmed for the overall reaction, which is consistent with all experimental observations.

## EXPERIMENTAL SECTION

UV–vis spectra and kinetic curves were recorded on scanning and diode-array spectrophotometers at a constant temperature maintained by the use of different thermostats with the various instruments. It was confirmed that photochemical effects do not interfere with the studied reaction in the diode-array spectrophotometers.[51] All measurements were performed at 25.0 ± 0.1 °C except for the temperature dependence studies. Standard 1.000 or 0.500 cm quartz cuvettes were used.

The pH-metric and iodometric measurements were taken with an automatic titrator. The pH electrode was calibrated by two buffers according to IUPAC recommendations.[47] The pH readings were converted to hydrogen ion concentrations as described by Irving et al.[52] The procedure and the evaluation of the titrations in determining the temperature dependence of the $pK_a$ of phen were conducted as described by Szabó et al.[46]

Electrospray ionization mass spectrometric (ESI-MS) analysis was performed in positive ion mode. The mass spectra were calibrated using the exact masses of the clusters generated from the electrosprayed solution of sodium trifluoroacetate (NaTFA).

$^1$H NMR spectra were measured at 400 MHz. The solutions were prepared in $H_2O$, and DSS (4,4-dimethyl-4-silapentane-1-sulfonic acid) in $D_2O$ was added to the sample in a capillary as an external standard for $^1$H (0 ppm). The $^1$H NMR spectra were recorded by using the standard watergate pulse sequence for the suppression of the water proton signal. In each experiment, 32 scans were collected with 16K data points using a sweep width of 5995 Hz, a pulse angle of 90°, an acquisition time of 1.366 s, and a relaxation delay of 1 s.

Nonlinear least-squares fittings of the titration curves and the kinetic traces at a given wavelength were performed with Scientist.[53] The standard deviation of the calculated rate constants was <5% in every case. Linear algebraic decomposition of the spectral changes was performed with Matlab.[54] Multiple kinetic curves recorded in nearly neutral medium and under different initial reactant conditions were simultaneously evaluated with ZiTa.[49] The simulation of the spectra of


DOI: 10.1021/acs.joc.6b00641
J. Org. Chem. 2016, 81, 5345–5353

the spectrophotometrically distinguishable species was performed with Specfit.[50]

All chemicals used in this study were of analytical reagent grade, purchased from commercial sources, and used as received without further purification.

With the exception of a few kinetic runs, the ionic strength was kept constant by using an excess of sulfuric acid or by the addition of appropriate amounts of sodium nitrate or sodium sulfate in all experiments.

## ■ ASSOCIATED CONTENT

### Supporting Information

The Supporting Information is available free of charge on the ACS Publications website at DOI: 10.1021/acs.joc.6b00641.

Figures showing the determination of the stoichiometry, kinetic traces recorded under different initial conditions, spectral changes of the reaction, dependence of the pseudo-first-order rate constants ($k_{obs}$) on PMS concentration, UV−vis molar spectra of phen, Hphen$^+$, phenO, and HphenO$^+$, $^1$H NMR spectra of phen and Hphen$^+$, dependence of the $^1$H NMR spectra of phenO on pH, temperature dependencies of the oxidation pathways, ESI-MS spectra of phen$O_2$, calculated spectra of the intermediate (I) and the product (P) of the reaction, calculated concentration profiles of the species, and tables of the singular values of the time-resolved absorbance spectra, the rate constants of the reaction at various reactant concentrations, effects of ionic strength on rate, temperature dependencies of the p$K_a$ of Hphen$^+$, and rate constants of the two oxidation paths of the reaction (PDF)

## ■ AUTHOR INFORMATION


### Corresponding Author

*E-mail: beller.gabor@science.unideb.hu. Telephone: +36 52 512-900, ext. 22327. Fax: +36 52 518-660.


### Notes

The authors declare no competing financial interest.

## ■ ACKNOWLEDGMENTS

The authors thank the Hungarian Science Foundation (OTKA) for financial support under Grant NK 105156. The research was supported by the EU and cofinanced by the European Social Fund under project ENVIKUT (TÁMOP-4.2.2.A-11/1/KONV-2012-0043). Dr. Bernadett Kalmár-Biri and Tibor Nagy are gratefully acknowledged for their assistance with the ESI-MS measurements. This research was also supported by the European Union and the State of Hungary, cofinanced by the European Social Fund in the framework of the TÁMOP 4.2.4. A/2-11-1-2012-0001 'National Excellence Program'.

## ■ REFERENCES


(1) In aqueous solution, peroxomonosulfate ion is involved in acid−base equilibria. $H_2SO_5$ may only exist under very acidic conditions, and the equilibrium concentration ratio of $HSO_5^-$ to $SO_5^{2-}$ is determined by the actual pH. In this paper, the abbreviation PMS corresponds to the total concentration of the oxidant; distinction between the different protonated forms is made when it is required by the clarity of the presentation.

(2) Hussain, H.; Green, I. R.; Ahmed, I. *Chem. Rev.* **2013**, *113*, 3329−3371.

(3) Zhu, W.; Ford, W. T. *J. Org. Chem.* **1991**, *56*, 7022−7026.

(4) Moriyama, K.; Sugiue, T.; Nishinohara, C.; Togo, H. 2015, *J. Org. Chem.80*, 9132−9140.

(5) Parida, K. N.; Moorthy, J. N. *J. Org. Chem.* **2015**, *80*, 8354−8360.

(6) Zhang, M.-Z.; Ji, P.-Y.; Liu, Y.-F.; Guo, C.-C. *J. Org. Chem.* **2015**, *80*, 10777−10786.

(7) Wang, Z.; Bush, R. T.; Sullivan, L. A.; Chen, C.; Liu, J. *Environ. Sci. Technol.* **2014**, *48*, 3978−3985.

(8) Lou, X.-Y.; Guo, Y.-G.; Xiao, D.-X.; Wang, Z.-H.; Lu, S.-Y.; Liu, J.-S. *Environ. Sci. Pollut. Res.* **2013**, *20*, 6317−6323.

(9) Durante, R. J.; Lee, S. J.; Tufano, T. P.; Park, Y. C.; Lee, J. W.; Lee, S. Y.; Lee, H. K.; Lee, Y. J.; Jang, S. H. US20100252530, 2010.

(10) Lente, G.; Kalmár, J.; Baranyai, Z.; Kun, A.; Kék, I.; Bajusz, D.; Takács, M.; Veres, L.; Fábián, I. *Inorg. Chem.* **2009**, *48*, 1763−1773.

(11) Kalmár, J.; Lente, G.; Fábián, I. *Inorg. Chem.* **2013**, *52*, 2150−2156.

(12) Bellér, G.; Lente, G.; Fábián, I. *Inorg. Chem.* **2010**, *49*, 3968−3970.

(13) McCleverty, J. A.; Meyer, T. J. *Comprehensive Coordination Chemistry II*; Elsevier: Oxford, U.K., 2003; Vol. *1*, pp 25−39.

(14) Bencini, A.; Lippolis, V. *Coord. Chem. Rev.* **2010**, *254*, 2096−2180.

(15) Corey, E. J.; Borror, A. L.; Foglia, T. *J. Org. Chem.* **1965**, *30*, 288−290.

(16) Beer, R. H.; Jimenez, J.; Drago, R. S. *J. Org. Chem.* **1993**, *58*, 1746−1747.

(17) Anbu, S.; Shanmugaraju, S.; Kandaswamy, M. *RSC Adv.* **2012**, *2*, 5349−5357.

(18) Engel, Y.; Dahan, A.; Rozenshine-Kemelmakher, E.; Gozin, M. *J. Org. Chem.* **2007**, *72*, 2318−2328.

(19) Patil, M. *J. Org. Chem.* **2016**, *81*, 632−639.

(20) Chen, Y. N.; Fan, Y.; Ni, J. *Dalton Trans.* **2008**, *5*, 573−581.

(21) Linsker, F.; Evans, R. L. *J. Am. Chem. Soc.* **1946**, *68*, 403.

(22) Dickeson, J. E.; Summers, L. A. *Aust. J. Chem.* **1970**, *23*, 1023−1027.

(23) Wimmer, F. L.; Wimmer, S. *Org. Prep. Proced. Int.* **1983**, *15*, 368−369.

(24) Kumar, R.; Mathur, P. *RSC Adv.* **2014**, *4*, 33190−33193.

(25) Mirífico, M. V.; Svartman, E. L.; Caram, J. A.; Vasini, E. J. *J. Electroanal. Chem.* **2004**, *566*, 7−13.

(26) Balicki, R.; Golinski, J. *Synth. Commun.* **2000**, *30*, 1529−1534.

(27) Kianmehr, E.; Rezaeefard, M.; Rezazadeh Khalkhali, M.; Khan, K. M. *RSC Adv.* **2014**, *4*, 13764−13767.

(28) MacCoss, M.; Ryu, E. K.; White, R. S.; Last, R. L. *J. Org. Chem.* **1980**, *45*, 788−794.

(29) Martins, A. F.; Eliseeva, S. V.; Carvalho, H. F.; Teixeira, J. M. C.; Paula, C. T. B.; Hermann, P.; Platas-Iglesias, C.; Petoud, S.; Tóth, É.; Geraldes, C. F. G. C. *Chem. - Eur. J.* **2014**, *20*, 14834−14845.

(30) Chavez, D. E.; Hiskey, M. A.; Naud, D. L. *Propellants, Explos., Pyrotech.* **2004**, *29*, 209−215.

(31) Farahani, M. D.; Honarparvar, B.; Albericio, F.; Maguire, G. E. M.; Govender, T.; Arvidsson, P. I.; Kruger, H. G. *Org. Biomol. Chem.* **2014**, *12*, 4479−4490.

(32) Murase, I. *Nippon Kagaku Zasshi* **1956**, *77*, 682−685.

(33) Wenkert, D.; Woodward, R. B. *J. Org. Chem.* **1983**, *48*, 283−289.

(34) Case, F. H. *J. Org. Chem.* **1962**, *27*, 640−641.

(35) Maerker, G.; Case, F. H. *J. Am. Chem. Soc.* **1958**, *80*, 2745−2748.

(36) Gillard, R. D. *Inorg. Chim. Acta* **1989**, *156*, 155.

(37) Rozen, S.; Dayan, S. *Angew. Chem., Int. Ed.* **1999**, *38*, 3471−3473.

(38) Carmeli, M.; Rozen, S. *J. Org. Chem.* **2005**, *70*, 2131−2134.

(39) Peintler, G.; Nagypál, I.; Jancsó, A.; Epstein, I. R.; Kustin, K. *J. Phys. Chem. A* **1997**, *101*, 8013−8020.

(40) Lente, G. *Deterministic Kinetics in Chemistry and Systems Biology*; Springer: New York, 2015; pp 48−53, 78−79.

(41) Ball, D. L.; Edwards, J. O. *J. Am. Chem. Soc.* **1956**, *78*, 1125−1129.

(42) Simon, A.; Ballai, Cs.; Lente, G.; Fábián, I. *New J. Chem.* **2011**, *35*, 235−241.




DOI: 10.1021/acs.joc.6b00641
*J. Org. Chem.* 2016, 81, 5345−5353

(43) Bretti, C.; Crea, F.; De Stefano, C.; Sammartano, S. *Fluid Phase Equilib.* **2008**, *272*, 47−52.
(44) Ishiguro, S.; Wada, H.; Ohtaki, H. *Bull. Chem. Soc. Jpn.* **1985**, *58*, 932−937.
(45) Summers, L. A. *Adv. Heterocycl. Chem.* **1978**, *22*, 1−69.
(46) Szabó, K.; Nagypál, I.; Fábián, I. *Talanta* **1983**, *30*, 801−804.
(47) Covington, A. K.; Bates, R. G.; Durst, R. A. *Pure Appl. Chem.* **1983**, *55*, 1467−1476.
(48) Galajda, M.; Fodor, T.; Purgel, M.; Fábián, I. *RSC Adv.* **2015**, *5*, 10512−10520.
(49) Peintler, G. *ZiTa: A comprehensive program package for fitting parameters of chemical reaction mechanisms*, version 4.1; Institute of Chemistry JATE: Szeged, Hungary, 1997.
(50) *Specfit/32, Global Analysis System*, version 3.0; Spectrum Software Associates: Marlborough, MA, 2004.
(51) Fábián, I.; Lente, G. *Pure Appl. Chem.* **2010**, *82*, 1957−1973.
(52) Irving, H.; Miles, G.; Pettit, L. D. *Anal. Chim. Acta* **1967**, *38*, 475−488.
(53) *Scientist*, version 2.0; Micromath Software: Salt Lake City, 1995.
(54) *MatLab for Windows*, version 4.2c1; The Mathworks, Inc.: Natick, MA, 1994.



DOI: 10.1021/acs.joc.6b00641
*J. Org. Chem.* 2016, 81, 5345−5353